Effects of solid and porous splitter plates located in the wake of a circular cylinder at Reynolds number Re = 800

S. KHANAL [a,*], L. FIABANE [a], D. HEITZ [a,b]

a. Univ Bretagne Loire, UR OPAALE, Irstea, F-35000 Rennes, France.
b. Univ. Bretagne Loire, Equipe Inria-Irstea Fluminance, F-35042 Rennes, France.
∗ Author to whom correspondance should be addressed : suman.khanal@irstea.fr

Résumé :

Un ensemble de configurations constituées de plaques séparatrices et d'un cylindre circulaire ont été testés comme déclencheurs géométriques pour générer des instabilités dans un flux d'air uniforme au nombre de Reynolds Re = 800 avec le but d'étudier à terme le rôle de la turbulence sur le dépot des particules. Deux types de plaques séparatrices (plaques pleines et grilles) de même dimensions sont utilisées. Les plaques séparatrices sont fixées au cylindre ou situées dans le sillage du cylindre, ce qui a permis de créer différentes instabilités. Les résultats préliminaires de ces configurations donnent un aperçu de la topologie d'écoulement et de la distribution spatiale du niveau de turbulence.

Abstract :

A set of configurations consisting of a circular cylinder and splitter plates have been tested as geometrical triggers to generate instabilities in an uniform airflow at Reynolds number Re = 800 with a further goal to study the role of turbulence on particles settling. Two types of splitter plates (solid plates and grids) of same size are used. The splitter plates are either attached to the cylinder or located in the wake of the cylinder which enabled to create different large-scale structures. Flow statistics obtained using a standard PIV setup provide an insight into the flow topology and the corresponding level of turbulence therein.

Keywords : Cylinder wake, Large scale structures, Splitter plates

1 Introduction

The transport and settling of small particles in airflows has been a subject of wide interest for some years now, as it is a crucial issue in many fields of research, from the dispersion and the destination of airborne pollutants, to the deposition of drugs deep in the lungs. Refined models for the particle trajectories exist (see e.g. [1] and references therein). Even though many terms of the models have been corroborated using numerical and/or experimental studies, some uncertainties remain. One of them is a precise and quantitative description of the effect of turbulent diffusion.

We tackle this challenging issue thanks to an experimental study that involves multiple interactions between particles, turbulent flow and passive obstacles and surfaces. The present proceeding deals with preliminary results on the flows we were able to produce, that will then be used to study particle deposition. We focus on two main aspects of the flow : the turbulence level through the velocity fluctuations, and the large scale structures in the flow, with the idea that the two could play a role on particle deposition.

As it has been the subject of many studies for its geometrical simplicity combined with the deep complexity of the flow it generates, we choose to use a circular cylinder as the geometrical trigger of instabilities in an otherwise laminar flow. It is well known that in viscous fluids past a certain velocity, the boundary layers created at the surface of a bluff body separates and create a wake downstream (see e.g. [3]). The non-dimensional parameter of choice to characterize the wake is the Reynolds number Re. In the case of the flow past a circular cylinder, the Reynolds number can be defined as :

$$Re = \frac{U_\infty D}{\nu}, \tag{1}$$

where U_∞ is the inlet flow velocity, D is the cylinder diameter and ν is the kinematic viscosity of the fluid (air in our case). From Reynolds numbers in between 40 and 50, the shear layers becomes unstable and roll-up to form vortices that are periodically shed in the wake, constituting the well-known von Kármán street. Up to $Re = 200$, the wake is mostly two dimensional ; when the Reynolds number is further increased up to 300, secondary vortices appear in the spanwise direction [2]. The boundary layer over the cylinder surface remains laminar, however, increasing Reynolds number over a very wide range, namely $300 < Re < 3 \times 10^5$. This regime is known as the subcritical flow regime. We set our study in this framework, choosing a Reynolds number of $Re = 800$.

In addition to the cylinder wake studies, many works have addressed the issue of controlling or even suppressing the shedding by means of passive controls such as splitter plates ([3], [4], [5]). A splitter plate is a thin, flat two-dimensional plate attached to the bluff body so that it splits the wake. It has been shown that these plates can prevent the interaction of the shear layers on each side of the cylinder so that it modifies the vortex shedding process (delay, shedding frequency, vorticity intensity).

In the present study, an experimental investigation was carried out in the near wake of a circular cylinder to study the effect of solid and porous splitter plates mounted on the wake centreline. The splitter plates are either attached to the cylinder or placed farther downstream. The production and spatial distribution of different level of turbulence compared to the case of the naked cylinder is analysed.

2 Experimental setup

2.1 Wind tunnel and PIV setup

The wind tunnel used in the experiments is a closed-loop, low-speed return wind tunnel. The sketch of the wind tunnel and its different parts along with the optical setup are shown in Figure 1.

The test section is 1400 mm long with an 280 mm square cross section at the inlet of the test section. The upper and lower walls of the test section are actually made slightly diverging to compensate for the boundary layer effects on the mean flow. This means that at the end of the test section, the square section height is close to 300 mm. For practical purpose, the width is kept constant.

Air is mixed and homogenized with seeding particles (oil droplets with diameter of approximatively 2 μm) inside the mixing chamber. It is driven by the fan towards the test section and through the fan, and

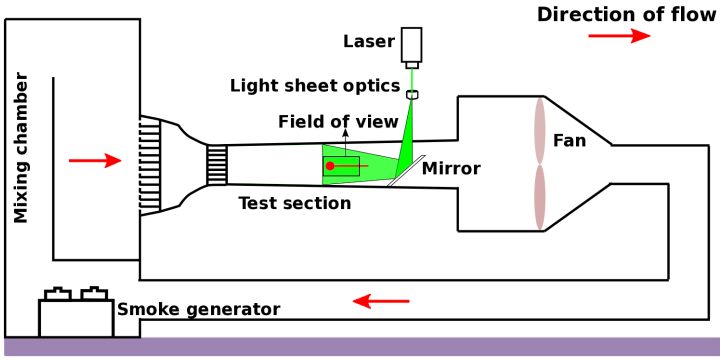

FIGURE 1 – Sketch of the wind tunnel with the PIV setup

then returned to the mixing chamber and back towards the test section (see red arrows in Figure 1). It yields a continuous circulation with a fairly constant concentration in particles.

The flow towards the test section is made uniform and without any global rotation thanks to two honeycombs located at the entrance and at the exit of the contraction section.

The PIV arrangement gives access to two in-plane velocity components that are measured in a plane field. The light source used is a New Wave Nd :YAG laser Solo III, with an energy pulse of 50 mJ and a wavelength $\lambda = 532$ nm. A system of mirrors and lenses is used to generate a millimetric vertical laser sheet in the middle of the windtunnel at the plane z=0 (Figure 1). A thin mirror of 7 mm width has to be installed inside the test section to minimize the shadows. Its effect on the flow was measured and found negligible within the PIV field of view location (distance upstream the mirror of twice its height and a hundred times its width).

The image acquisition is performed by a PCO camera SensiCam located perpendicularly on one side of the laser sheet. The camera sensor is of CCD type with a resolution of 1280 $\times$ 1024 pixels and a dynamics of 12 bits. The camera is equipped with a 50 mm focal length lens, set at an aperture of 5.6. It is located at a distance of around 700 mm, yielding a field of view of 110 mm $\times$ 90 mm and a pixel size of around 6.7^2 μm^2.

2.2 Flow configurations

A circular cylinder of diameter $D = 15$ mm and width 280 mm was installed in the wind tunnel to create instabilities and flow structures. The inlet flow velocity was fixed to $U_\infty = 0.8$ m/s, yielding a Reynolds number based on the cylinder diameter of $Re = U_\infty D/\nu_{\text{air}} = 800$. A plane plate (length $L = 112$ mm, width 280 mm, thickness 2 mm) was added in the wake of the cylinder at different locations. It is referred to as the splitter plate in the rest of the proceedings. The splitter plate length L is quite long compared to the cylinder diameter : $L/D \approx 7.5$.

Two types of splitter plates were used : solid plates and grids, to study the possible effect of the collecting surface porosity on the flow and subsequently on the particle deposition. The grid used had a square opening of 245 μm (Figure 2), with dimensional parameters summarized in Table 1.

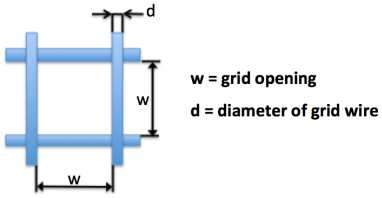

FIGURE 2 – Sketch of the grid

grid size w (mm)	diameter of the grid wire d (mm)	Porosity $\epsilon = w^2/(w+d)^2$
0.245	0.065	62%

TABLE 1 – Parameters of the grid used

The splitter plates were located in the wake centerline at different distances downstream of the cylinder. The large-scale flow dynamics as well as the local velocity fluctuations were then studied.

2.3 Data acquisition and post-treatment

We performed PIV measurements for the flow around the cylinder without any splitter plate as a reference, then for the flow around the different configurations with porous or plain splitter plates. The post-treatment was done using the commercial software DaVis 8.3 : the vector fields were computed using a cross-correlation technique with decreasing interrogation windows (64 $\times$ 64 down to 12 $\times$ 12) and a 50 % overlapping. The time delay between two laser pulses was $\Delta t = 1000\mu$s. The frequency of the image acquisition was 4 Hz which was lower than the vortex shedding frequency for the circular cylinder wake at Re = 800 which was calculated to be around 12 Hz. This means that : (i) the velocity fields are not time-resolved ; and (ii) that the instantaneous fields are independent. An ensemble of 2000 independent image pairs was acquired for each experiment which was verified to be sufficient to obtain converged mean flow statistics.

The results are presented using two quantities : the vorticity and the Turbulent Kinetic Energy (TKE).

Vorticity is defined as the curl of the flow velocity : $\vec{\omega} = \nabla \times \vec{u}$, where ∇ is the classical del operator. In two dimensional flows (velocity in the x-y plane, as obtained using a single camera), the vorticity vector is always perpendicular to the plane and can be expressed as a scalar field :

$$\omega_z = \frac{\partial v}{\partial x} - \frac{\partial u}{\partial y}. \tag{2}$$

Instantaneous vorticity fields allow to visualize the flow structures in the wakes of the different configurations.

Turbulent kinetic energy (TKE), noted k, is the mean kinetic energy per unit mass associated with vortices in a turbulent flow. It is defined using the velocity fluctuations u_i' and usually quantified by the mean of the turbulent normal stresses : $k = \left(\overline{(u')^2} + \overline{(v')^2} + \overline{(w')^2}\right)/2$, where the upper bar denotes the time averaging. High TKE therefore points to regions where there are eddies with higher energy content. For two dimensional vector fields, that is with no z-component w, DaVis uses for the missing component the mean of the other two components [6], yielding :

$$k = \frac{3}{4}\left(\overline{(u')^2} + \overline{(v')^2}\right). \tag{3}$$

This assumption gives a similar result as a "two dimensional" TKE, with an added prefactor. It is known that the eddies are only slightly three dimensional in this range of Reynolds numbers REF, meaning the contribution of z-velocity fluctuations should be negligible. Hence, the prefactor overestimates the TKE but with no changing in the TKE topology : the comparison between different configurations still stands.

Note that all the results have been normalized using U_∞ and D, respectively as velocity and length scales.

3 Results and Discussion

3.1 Reference : flow past a cylinder

Results for the instantaneous vorticity and the TKE in the flow past a cylinder without any splitter plates are shown in Figure 3 and used as a reference.

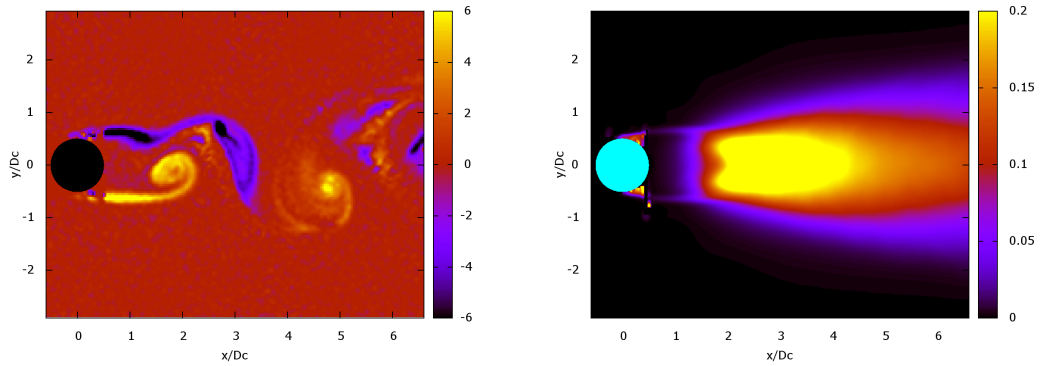

(a) (b)

FIGURE 3 – (a) Instantaneous vorticity, and (b) Turbulent Kinetic Energy, in the flow past a cylinder

As explained in the introduction, we can observe the expected vortex shedding behind the cylinder at this Reynolds number of 800 (Figure 3a). Two boundary layers separates from both the top and bottom surfaces of the cylinder to form shear layers which are highly unstable and periodically roll-up into vortices. Looking at the mean velocity, it is possible to define a so-called recirculation region : it is the area immediately behind the cylinder where the flow direction reverse. A way to estimate the distance between the cylinder base and the vortex formation is therefore to compute the recirculation bubble length L_f [7], defined from the downstream stagnation point of the mean flow located on the centerline. In our case we observe $L_f/D = 2.3$.

The end of the vortex formation region is followed by a transition region marked by a peak in the TKE, with a maximum of $k_{\text{max}} = 0.3$ located slightly farther downstream the formation length at $x/D \approx 2.5$, on the centerline (Figure 3b). This is due to the alternate shedding of energetic vortices that induce large velocity fluctuations locally. The flow close to the cylinder is quite stable, with only a small motion of the shear layers correlated with the shedding, and contains a small TKE. Once shed, the vortices diffuse as they are advected downstream and partly dissipate ; it results in a more spread TKE.

It can be seen on both Figures 3a and 3b that some data are missing in the close vicinity of the cylinder, due to laser reflections on the cylinder surface. We masked the incriminated areas in the images to prevent outlier vectors. Since the area of interest in our case is the wake of the cylinder, this issue is not seen as crucial. Nevertheless it yields non-symmetrical min-max values for the mean vorticity, which is in the range [-8.9, 8.3].

3.2 Splitter plate attached to the cylinder

As mentioned in section 2.2, two types of splitter plates were attached to the back of the cylinder. Results of vorticity and TKE are shown in Figure 4 for both types, with grids in light colors (Figures 4a and 4b) and solid plates in dark colors (Figures 4c and 4d).

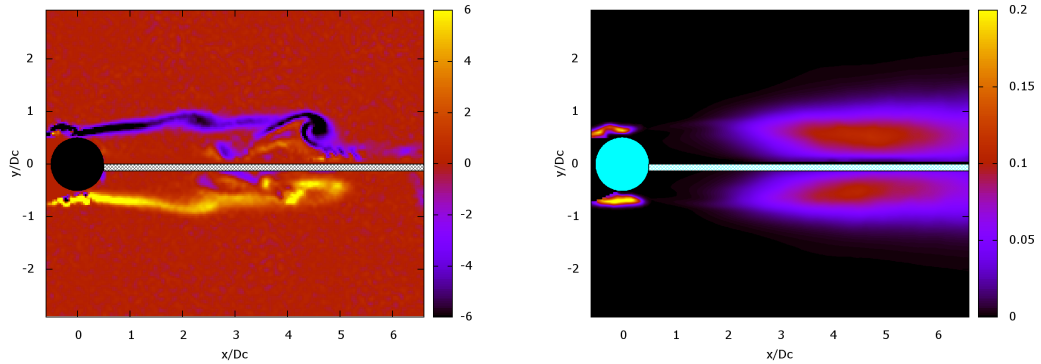

(a) Vorticity, grid attached to the cylinder

(b) TKE, grid attached to the cylinder

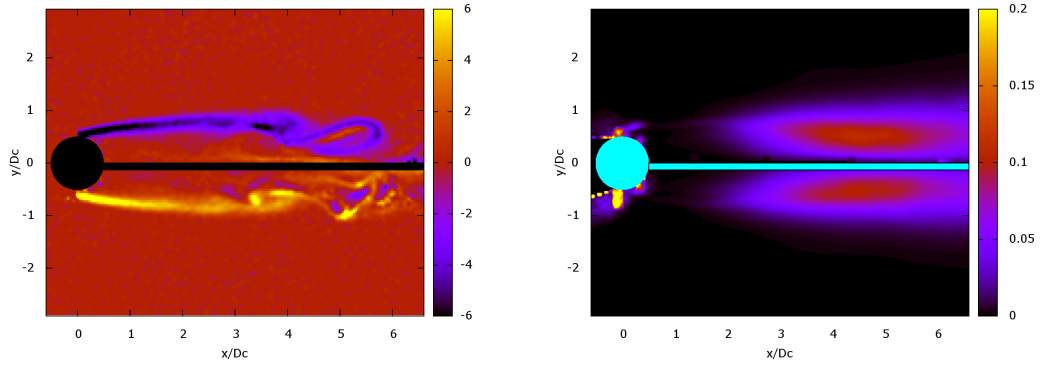

(c) Vorticity, solid plate attached to the cylinder

(d) TKE, solid plate attached to the cylinder

FIGURE 4 – Instantaneous vorticity fields and TKE for splitter plates attached to a cylinder

Both configurations look the same. In Figures 4a and 4c the shear layers are more elongated than in Figure 3a, with a vortex formation length of 4.8 (that is more than twice as large as in the case of a naked cylinder). This is in accordance with the literature (e.g. [3, 4]) for long splitter plates ($L/D > 5$) attached to a cylinder. The mean vorticity has similar extremum levels in the range [-8.9, 7.9], with again non-symmetrical values. On both sides of the splitter plate, the shear layers roll up downstream into vortices which then impact the splitter plates to break into smaller structures.

Looking at the TKE (Figures 4b and 4d), both configurations give very similar results in terms of TKE levels and peak locations. The peaks are located close to the formation length at $x/D = 4.7$ for the grid and $x/D = 4.5$ for the solid plate. Again, this is where the shear layers roll up, inducing energetic vortices that then diffuse. Contrary to the naked cylinder, there is no alternate shedding and the vorticity keeps its sign on each side of the splitter plate. This yields smaller values of the TKE, with $k_{\max} \approx 0.1$. The wake seems also thiner in the case of the attached splitter plate as the vortices travel along the plate. They seem to diffuse less in the presence of a plate than when freely advected downstream in a cylinder wake.

The shedding and temporal evolution of large scale vortices seem to be similar on both sides, yet no clear link (temporal or spatial) between the upper and lower shedding can be drawn. In particular, no flux could be observed through the porous splitter plate on our different results (instantaneous or mean fields, velocity and its spatial derivatives). It is unclear whether this lack of observation is due to the resolution or to the physics. Ref. [8] claims that the matter flux through a grid is almost inexistent past a certain grid solidity, but suggests that possible synchronization of the shedding can be achieved through the pressure field. This specific point will be investigated through future time-resolved PIV experiments.

In the current state of our study, the conclusion is that the two configurations resemble most a backward facing step flow, with two distinct recirculation regions located at upper and lower sections separated by the plates. It is not possible with our results to identify clear differences between porous and solid plates. However the addition of the splitter plate permitted the production of different level of turbulence compared to the case of the naked cylinder.

3.3 Splitter plate in the wake of the cylinder

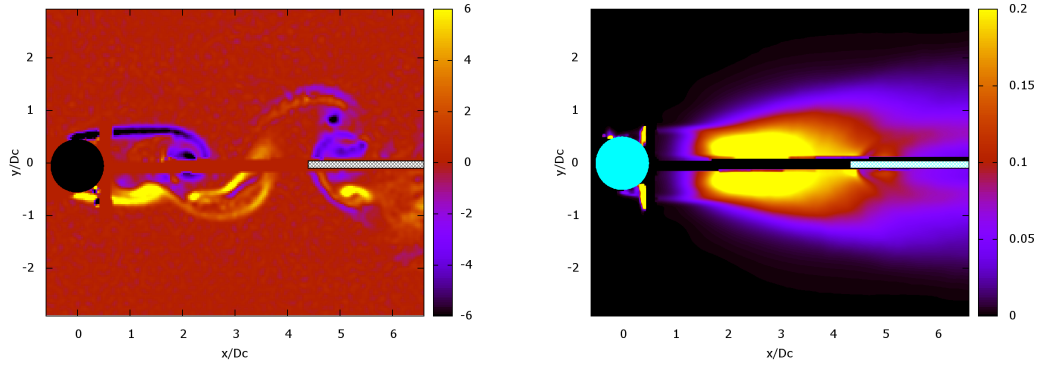

(a) Vorticity, grid placed in the cylinder developed wake

(b) TKE, grid placed in the cylinder developed wake

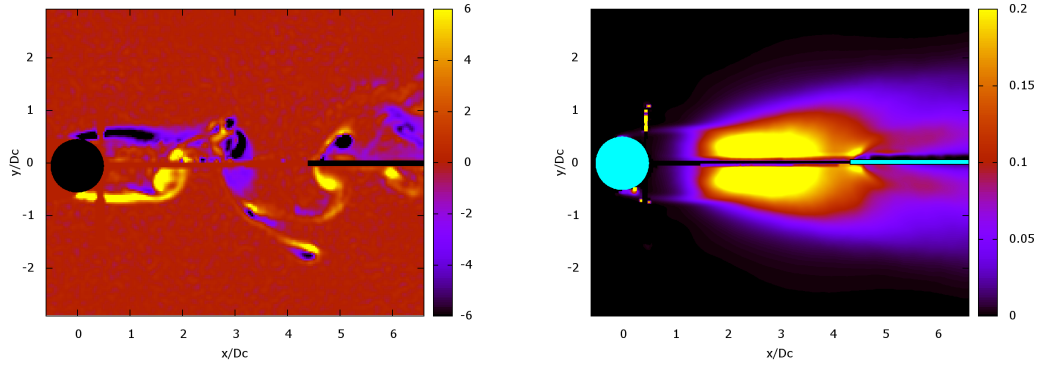

(c) Vorticity, solid plate placed in the cylinder developed wake

(d) TKE, solid plate placed in the cylinder developed wake

FIGURE 5 – Instantaneous vorticity fields and TKE of splitter plates in the developed wake of a cylinder

The splitter plates were then detached and located in the wake of the cylinder. The first location was fixed close to the formation length of the naked cylinder, that is the leading edge of the splitter plate

was at $x/D = 2$. Placing the splitter plates at a distance $2D$ from the cylinder did not change the flow compared to the case with attached plates (results not shown here). The Von Karman vortex street was suppressed and the vortex shedding delayed as in section 3.2. This is in accordance with the literature (see e.g. [7]).

The splitter plate was then placed farther downstream at $x/D = 4$. Results are shown in Figure 5. In this configuration it can be observed that the vortex shedding happens between the cylinder and the splitter plate. The flow can be therefore decomposed as a cylinder wake flow that impacts a plane plate : a von Kármán street is created and interacts with the leading edge of the plate, creating secondary vortices of smaller sizes (Figures 5a and 5c). The formation length of the cylinder wake is only slightly modified by the presence downstream of the splitter plate, with $L_f/D = 2.4$. The mean vorticity spans however a wider range of values comprised in [-16.1, 14.7], which is not yet fully understood.

Figures 5b and 5d show the TKE, that can also be decomposed into two parts. The part between the cylinder and the plate is much similar to the results for a naked cylinder, with $k_{\text{max}} \approx 0.3$ at $x/D \approx 2.5$ Then the shed vortices encounter the plate, creating fluctuations and therefore TKE at the splitter plate leading edge. The part of the flow surrounding the detached plate is more turbulent than its counterpart surrounding the attached splitter plate.

As for the attached splitter plate configuration, no clear effect of the plate porosity is observed from our results. There is only a small discrepancy in the TKE at the leading edge of the splitter plate, that cannot be analyzed given the current resolution of the results. This point will be addressed in future experiments with higher resolution.

Références

[1] A. Guha, Transport and deposition of particles in turbulent and laminar flow, Annu. Rev. Fluid Mech, 2008

[2] M. S. Bloor, The transition to turbulence in the wake of a circular cylinder, Journal of Fluid Mechanics, 19(02) :290-304, 1964

[3] A. Roshko, On the wake and drag of bluff bodies, Journal of the aeronautical sciences, 22(2) :124-132,1955, 1955

[4] C. J. Apelt, G. S. West, The effects of wake splitter plates on bluff-body flow in the range 10^4< Re< 5×10^4. part 2, Journal of Fluid Mechanics, 71(01) :145-160, 1975

[5] M. F. Unal, D. Rockwell On vortex formation from a cylinder. Part 2. Control by splitter-plate interference, Journal of Fluid Mechanics, 19 :513-529, 1987

[6] Product-Manual for DaVis 8.3, LaVision GmbH, Anna-Vandenhoeck-Ring 19, D-37081 Gottingen, 2016

[7] J. H. Gerrard, The mechanics of the formation region of vortices behind bluff bodies, Journal of Fluid Mechanics, 25(02) :401-413, 1966

[8] G.S. Cardell Flow past a circular cylinder with a permeable wake splitter plate, Ph.D. Thesis, California Institute of Technology, 1993